APPLICATION OF A 3D NAVIER-STOKES SOLVER TO ANALYSE THE PERFORMANCE OF A LOBED MIXER

G. ROLLIN, J.L. DUPARCQ, H. JOUBERT

Snecma Villaroche Center 77550 Moissy Cramayel - France

Abstract

In order to achieve a good optimization of lobed mixers in turbofan engines, designers must take into account a great deal of parameters (number of lobes, lobe shape and degree of radial penetration...). This implies a satisfactory understanding of the complex aerodynamic phenomena occuring in the nozzle, which cannot be easily done with experimental way. The computational procedure described in this paper relies on the 3D Navier-Stokes code CANARI developped at ONERA. The numerical method is based on a finite volume approach with an explicit centered scheme. Turbulence is modeled using a Baldwin-Lomax model. The results presented show the ability of the code to simulate the flowfield, especially the strong streamwise vorticity generated by the mixer. Nevertheless, due to the simple turbulence model implemented, the mixing process seems to be underestimated.

Nomenclature

Cd	Mass flow coefficient
Cv	Thrust coefficient
NPR	Nozzle pressure ratio
p	Static pressure
V	Velocity
λ	By-pass-ratio
γ	Specific heat ratio
ρ	Density
μ_t	Turbulent viscosity
τ	Viscous stress tensor
τ_R	Reynolds stress tensor
ω	Vorticity

Subscripts

c	Core condition
f	Fan condition
e	External condition
t	Total value

Introduction

Lobed mixers have been often used in turbofan engines to improve internal mixing of the core-stream and the fan-stream before the nozzle exit station. The benefit of such a device is potentially wide : the increase of efficiency can be expressed in terms of specific fuel consumption and noise reduction. It is obvious now that these two features have become crucial for present and future civil aircrafts.

One of the problems raised in the design process of a mixer is the difficulty to find the right balance between the mixing efficiency and the level of additional pressure losses. Up to now, and maybe for some more years, due to the complexity of the lobed mixer geometries and to the state of the art in numerical simulations, the design of mixers have been carried out with empirical methods or numerous wind tunnel tests.

For industrial companies, the main drawback of this methodology is obviously that wind tunnel tests are generally time and money consuming. Furthermore, during experimental tests designers usually get information about the mixer global performances (mixing level, mass flow, thrust...) but very seldom about the origin of the mixing process itself. In that context, it is very hard to make significant progress in the design methodology.

An answer could be the implementation of a specific well-instrumented experiment on a realistic mixer. Two difficulties occur : the first one is that the regions where the mixing process is actually initiated are not very accessible (mixers are generally located upstream of the nozzle exit station), and the second difficulty is due to the kind of measurement needed (velocity, pressure, temperature and eventually turbulent quantities fields) which require a sophisticated instrumentation. Moreover, non-intrusive measurement techniques are necessary to have a fine description of the flowfield if one compares the common model scale size used in experiments with probes sizes.

The aim of the present study is not to propose an alternative to the current design process. Testing will always be necessary with regards to the number of physical phenomena occuring in the flowfield that cannot be correctly taken into account by the numerical simulations (turbulence, chemistry...). The approach presented herein should be seen as a new engineering tool offered to the designers in order to improve their understanding of the basic phenomena of the mixing process, and therefore to reduce the number of iterations in the global design process of a mixer.

Computational method

Numerical scheme

The analysis of the mixer and nozzle flowfield was performed using the 3D Navier-Stokes solver CANARI developped at ONERA [1,2] which features a cell-centered approach for multidomain structured meshes. Since this paper is not focused on the numerical aspect, we only briefly describe the solver in the following, with a special emphasis on the implementation of the turbulence model. Further detail can be found in the reference papers.

The equations to be solved are the Reynolds averaged continuity, momentum and energy equations written in the conservative form :

$$\frac{\partial \rho}{\partial t} + \operatorname{div}\left(\rho \overline{V}\right) = 0$$

$$\frac{\partial \rho \overline{V}}{\partial t} + \operatorname{div}\left(\rho \overline{V} \otimes \overline{V} + p\overline{\overline{I}}\right) = \operatorname{div}\left(\overline{\overline{\tau}} + \overline{\overline{\tau}}_R\right)$$

$$\frac{\partial \rho E}{\partial t} + \operatorname{div}\left(\rho E \overline{V} + p\overline{V}\right) = \operatorname{div}\left[\left(\tau + \tau_R\right).\overline{V} - \overline{q} - \overline{q}_t\right]$$

where $\overline{\overline{\tau}} = -2/3\mu\left(\operatorname{div}\overline{V}\right).\overline{\overline{I}} + 2\mu\overline{\overline{D}}$

In the previous equations, ρ represents the density, $\overline{V}$ the velocity and E the total energy. The static pressure is related to the energy through the equation of state given for a perfect gas by

$$p = (\gamma - 1)\left(\rho E - 1/2\rho\overline{V}^2\right)$$

The numerical solution of these equations is obtained using a time marching technique. The equations are discretized using a 4 steps Runge-Kutta space centered scheme which is second order time accurate in the inviscid zones and first order in the viscous zones.

In order to obtain a dissipative scheme, a fourth order linear dissipation is added. A second order non linear dissipation is also added to capture correctly the flow discontinuities.

An implicit stage proposed by Lerat [3] is used in CANARI. It preserves the space centered approach, the conservative property, the accuracy and the dissipative (or non dissipative) aspect of the explicit stage.

Turbulence modeling

The Reynolds stress tensor τ_R is modeled using the Boussinesq eddy viscosity approach which assumes a direct relationship between the turbulent momentum fluxes and the mean velocity gradients. By analogy with the expression for the viscous stress tensor, one writes :

$$\overline{\overline{\tau}}_R = -2/3\mu_t\left(\operatorname{div}\overline{V}\right).\overline{\overline{I}} + 2\mu_t\overline{\overline{D}}$$

$$\overline{\overline{D}} = 1/2\left[\Delta\overline{V} + \left(\Delta\overline{V}\right)^t\right]$$

Since the first term in the right hand side is neglectable, τ_R is expressed as follows :

$$\overline{\overline{\tau}}_R = \mu_t\left[\Delta\overline{V} + \left(\Delta\overline{V}\right)^t\right]$$

In this study, the main modification made to the code was a new implementation of the turbulence model with a three type zonal algebraic model. This was done because there are three types of distinct viscous regions : boundary layers near surfaces, shear layers downstream of trailing edges, and free-stream in regions away from any shear or boundary layer.

In boundary layers, turbulent viscosity is modeled by the classical Baldwin-Lomax model in its original formulation [4]. This is a two layer model that follows the pattern of Cebecci but avoids the necessity of determining the boundary layer thickness.

Because of the relative complexity of the flowfield dowstream of the mixer trailing edge, a simple mixing length model is used in region containing a shear layer.

The turbulent viscosity is given by

$$\mu_t = \alpha\rho\omega\delta^2(x)$$

with $\alpha = 0.001$

In the previous equations, ω represents the vorticity and ρ the density. The mixing length δ is derived from the distance from the trailing edge station d_{TE}, the estimation of the shear layer thickness at nozzle exit station δ_E, and a characteristic length of the geometry L.

$$\delta(x) = \delta_E.\mathrm{th}(d_{TE}/L)$$

The value of α was chosen in previous calculations performed on simpler geometries (axisymmetric shear layers) to get a realistic level of turbulent viscosity.

In regions away from any shear or boundary layer, the expression used for the turbulent viscosity is quite similar

$$\mu_t = \alpha\rho\omega l^2$$

The mixing length l is constant and depends on the free-stream turbulence intensity.

This turbulence model is obviously too simple to handle correctly all the phenomena related to turbulence (3D shear layer instabilities, noise...). Nevertheless it should be sufficient to provide an overall description of the flowfield.

Grid generation

Among all the problems raised by the numerical simulation of the flowfield in a lobed mixer, grid generation has often been identified as the main difficulty. As a matter of fact, the first computations on realistic mixer geometries only appear at the end of the 80's [5,6] whereas 3D calculations on others complex geometries such as compressor bladings were carried out before.

The explanation for this situation is the typical shape of a mixer. The topological decomposition is generally quite simple (fig. 1) ; the entire geometry may be divided into three or four blocks : the core-stream and the fan-stream ducts upstream of the mixer trailing edge station (blocks 1 and 2), the mixing region dowstream (block 3) and eventually a fourth block in order to take into account the external flow (block 4). The problem here comes from the evolution of the cross-section shape in the first two blocks with regards to the possibilties of the current mesh generators and to the numerical method used to simulate the flowfield.

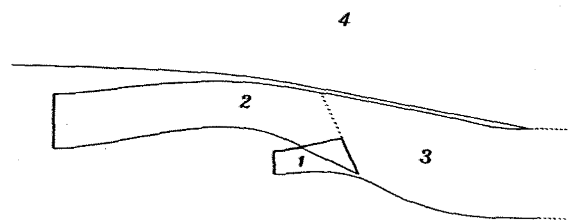

FIGURE 1 : Topological decomposition

It is generally recommended to generate a smooth grid with regular evolution of the cell sizes along all directions. More especially, minimum skewing should be introduced to the grid of each block. This is particularly true around the mixer where the grid generator has to be efficient enough to give a good resolution both in the middle of the core and fan ducts, and in the vicinity of the surfaces.

For the same reason, a particular attention has to be paid to the grid of the mixing region (block 3 in fig. 1), in order to ensure a good continuity of the cell size from both sides of the boundaries between the blocks.

For the Navier-Stokes simulations, the mesh density should to be increased in regions where strong gradients appear such as boundary or shear layers. In boundary layers, previous studies carried out with CANARI have pointed out the importance of the regularity control of the first cell near wall. In the grid described here after, the first cell size was set to 10 μm which corresponds to y^+ for the first grid point off the wall less than 3.

For this study, The Navier-Stokes type grid was built in four steps :

- Firstly, from the geometrical description of the mixer available on CATIA CAD system, the topological decomposition was achieved according to the sketch presented in figure 1. However to avoid a too strong discontinuity at the trailing edge mixer station, the mixing duct (block 3 in fig. 1) was divided into two blocks in the continuation of the core and fan ducts. Once the mesh is built, these two blocks will be gathered, and the calculation will be done with only one block in the mixing region.

- Secondly, the boundary surface meshes were generated. This step is not very difficult but it must be carried on very carefully because the wall meshes have a major influence on the final 3D mesh.

- Thirdly, the 3D Euler type mesh was built using transfinite interpolations(7). Several iterations are necessary between the wall mesh generation and the 3D interpolations to minimize skewing.

- And finally, for the Navier-Stokes applications, the grid density is locally increased where needed by linear interpolations.

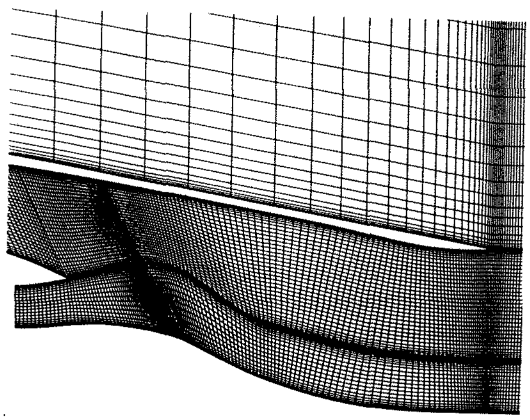

FIGURE 2 : Grid in the plane of symmetry

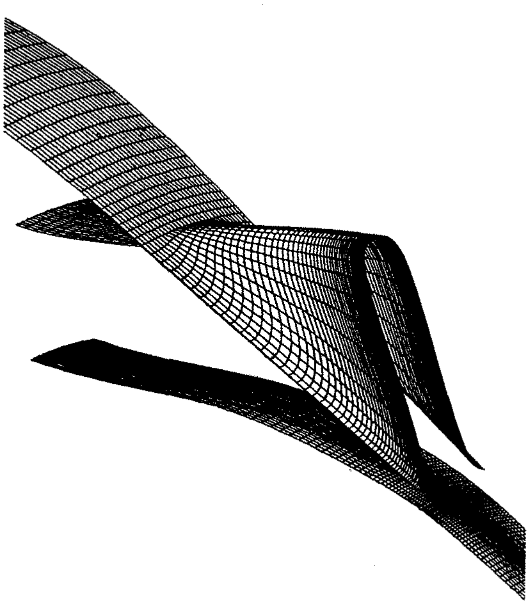

FIGURE 3 : Mixer wall grid

The result of the grid generation process is presented in fig. 2, 3 and 4. The computational domain is divided into 4 blocks (including external flow). The Euler type grid corresponds to 320.000 grid points, and the Navier-Stokes type grid 540.000 grid points.

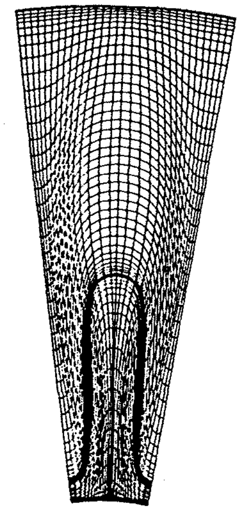

FIGURE 4 : Mixer Trailing edge grid

Boundary conditions

The boundary conditions require for the Euler or Navier-Stokes calculations are the total pressure and temperature distributions, the velocity direction for the inflow boundaries (core-stream, fan-stream and external flow), and the static pressure for the outflow boundaries. The total pressure and temperature are supposed to be constant at the charging stations except in the boundary layer. For lack of experimental data, the thickness of the boundary layers were set to 10 mm for the internal charging stations, and to 25 mm for the external upstream boundary. The total pressure and temperature profiles were derived from outer conditions with a modified Crocco law.

At the outflow boundaries of the computational domain, the static pressure is constant and equal to the external upstream static pressure. This assumption means that the external boundaries are far enough to neglect the perturbations due the nozzle.

At the mixer and nozzle wall, zero velocity, zero normal pressure and temperature gradient are specified.

The calculations performed on three distinct thermodynamic conditions (see table 1), were based either on inviscid flow assumption (Euler equations) or on viscous flow assumption (Navier-Stokes equations). The first three cases correspond to take-off conditions with a low external Mach number (M_e=0.3) and the last one correspond to cruise condition. In this case, the flow is supersonic at the nozzle exit station ; therefore, the computation was carried out without taking into account the external flow.

Case	NPR_c	NPR_f	M_e	Hyp.
I.E	1.55	1.64	0.3	Euler
II.E	1.51	1.60	0.3	Euler
II.N	1.51	1.60	0.3	N. S.
III.N	2.30	2.42	-	N. S.

TABLE 1 : thermodynamic conditions

Results

The calculations were performed on a CRAY YMP. The convergence criterium chosen was based on the mass flow rate conservation in the mixing region (when convergence was reached, the variations of the mass flow rate did not exceed 0.2 % or 0.3 %). The total CPU time required for the Navier-Stokes calculations was about 10 hours.

Flow structure

The very first qualitative result obtained in this study is that whatever thermodynamic conditions we chose for our calculations, the flow structure computed had the same feature. The flow structure in the nozzle is mainly driven by the total pressure and temperature ratios between core-stream and fan-stream. From one to another case, these ratios are quite the same. For a rather wide range of conditions, the external flow has a minor influence on the internal flow pattern.

From the particule traces shown in figure 5 we can point out the typical features of the flowfield, and first of all, the strong streamwise vorticity generated by the mixer. It seems clear that these vorticies are generated by the radial deflection of the core and the fan streams at the mixer trailing edge station. The contribution of the three-dimensional instabilities in the shear layer is weaker. As a matter of fact, the comparison presented in figure 6 between the velocity fields at the nozzle exit station computed either by an Euler approach (left hand side) or by a Navier-Stokes approach (right hand side) shows that there is no qualitative difference in the flowfield

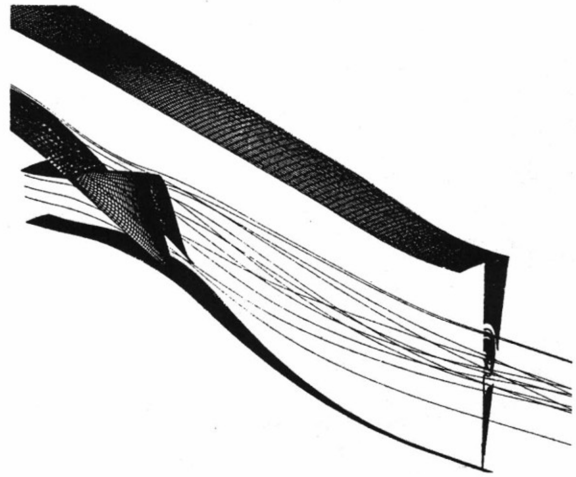

FIGURE 5 : Particule traces in the nozzle (case II.N)

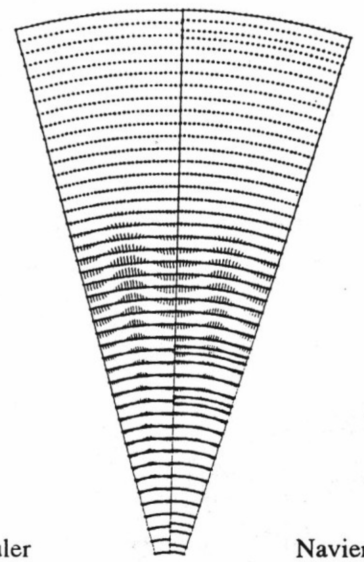

FIGURE 6 : Velocity fields at the exit nozzle station (cases II.E and II.N)

The particule traces in the wall mixer vicinity (fig. 7) indicate that for this particular lobed mixer geometry, no separation occurs in spite of an important pressure gradients. However, due to the obstruction of the upper wall mixer , the deflection of the fan stream lines is very important. The same phenomenum occurs with the core stream lines, but the flow is deflected in the other side. As mentioned before, these defections create the strong streamwise vorticity downstream of the mixer trailing edge. Moreover there influence on the boundary layer behavior is far from being negligible (fig. 8).

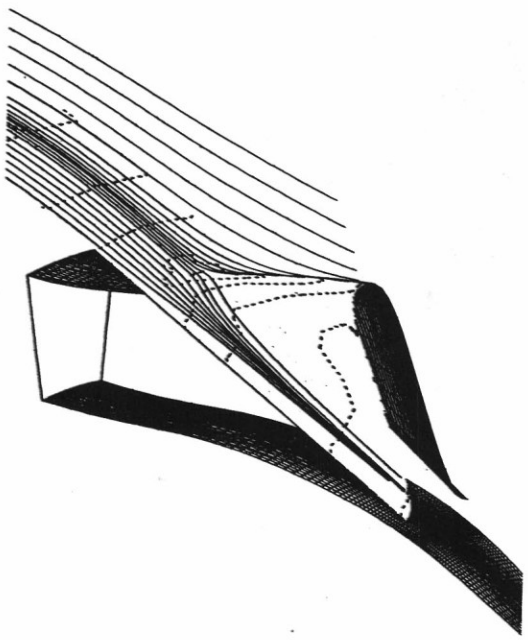

FIGURE 7 : Fan stream lines in the mixer vicinity (case II.N)

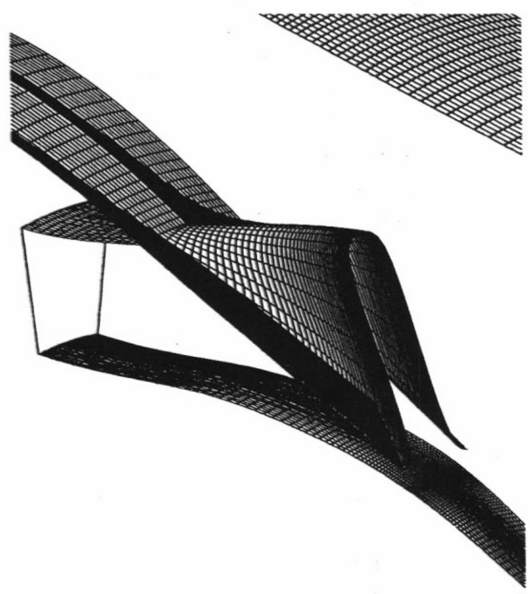

FIGURE 8 : Boundary layer evolution (case II.N)

The pair of vortices generated by the mixer lobe provides the mixing between the core-stream and the fan-stream. Figure 9 shows the evolution of the total temperature contour plots in cross-sections along the mixing duct. The vortices described below result in a typical "horse-shoe shaped total temperature signature" at the nozzle exit station. This phenomenum is captured either by the Euler computational or by the Navier-Stokes computation (fig. 10).

The mixing level computed according to the Euler or Navier-Stokes approach is quite similar. This comes from the simple turbulence model implemented in the code. The contribution of turbulence in the mixing process is for sure underestimated.

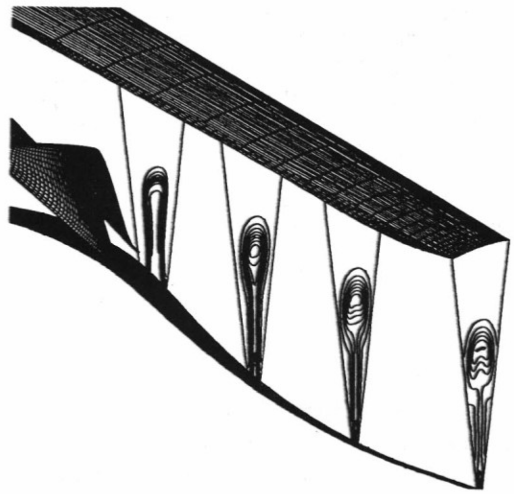

FIGURE 9: Total temperature contour Plots (case II.N)

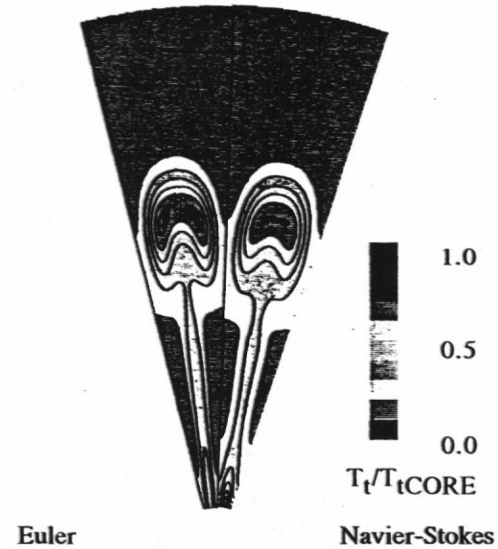

FIGURE 10 : Total temperature contour plots at nozzle exit station (cases II.E and II.N)

Nozzle performance analysis

The purpose of this flowfield simulation around the mixer is also to get an overall estimation of the nozzle performance. In the design process, several non-dimensional parameters are used to characterize the nozzle performances.

- the bypass ratio :

$$\lambda = \frac{\dot{m}_{ACTUAL}(FAN)}{\dot{m}_{ACTUAL}(CORE)}$$

- the mass flow coefficient :

$$C_D = \frac{A_{FM\ EFF}}{A_{GEOM}}$$

with $$A_{FM\ EFF} = \frac{\Sigma(M_{IDEAL})}{K^*} \frac{\dot{m}_{ACTUAL}\sqrt{T_{T\ MIX}}}{P_{T\ MIX}}$$

- and the thrust coefficient :

$$C_V = \frac{F_{ACTUAL}}{V_{IDEAL}\dot{m}_{ACTUAL}}$$

In the previous definitions, $P_{T\ MIX}$ and $T_{T\ MIX}$ are the fully-mixed total pressure and temperature at the nozzle throat station, $A_{FM\ EFF}$ is the fully-mixed effective section area, A_{GEOM} is the nozzle exit section area for unchoked conditions and the nozzle throat area for choked conditions, and V_{IDEAL} and M_{IDEAL} are the velocity and the Mach number of the flow isentropically expanded from the nozzle exit.

For the various thermodynamic conditions, the computed performances are presented in table 2.

CASE	λ	C_D	C_V
I.E	7.97	0.996	0.964
II.E	8.02	0.995	0.957
II.N	7.97	0.984	0.954
III.N	7.67	0.991	0.982

TABLE 2 : Nozzle performances

Waiting for further validation, we can make three preliminary comments on these results. First of all we can note that the levels of the predicted coefficients seem realistic. More precisely, the simulation provides the right trends between unchoked and choked conditions. Secondly, the influence of viscous effects on the mass flow coefficient is quite obvious if one compares case II.E and case II.N. And finally, for the same two cases, there is no difference between the computed thrust coefficients. This last point shows that the contribution of viscous effects on the mixing process is underestimated in the code, the thrust coefficient should have increased when taking into account turbulence. A significative improvement in turbulence modeling is necessary in order to get a more precise estimation of Cv.

Conclusions

The results obtained by the use of a 3D Navier-Stokes code have shown the ability of this approach to simulate the flowfield in a turbofan engine nozzle equipped with a lobed mixer. The whole aerodynamic phenomena occuring in the nozzle have been reproduced, and mainly the strong streamwise vorticity generated by the mixer which is the origin of the mixing process.

This methodology based on numerical simulations has become now an efficient engineering tool which has been used at Snecma for the design of new mixers. It enables the designers to make the necessary compromise between the mixing efficiency, the pressure losses and the acoustic behavior (expressed in terms of velocity profiles at the nozzle exit station).

Nevertheless, in order to improve the flowfield prediction, especially to be able to reproduce the right mixing level, a more realistic turbulence model should be implemented in the code.

Acknowlegments

This study has been conducted at Snecma Engineering. The authors are grateful towards to Aerodynamic Integration Department staff who supported them during this work. We also express our thanks to Snecma General Managment for authorizing this publication.

References

[1] Couaillier V., Veysseyre Ph., Vuillot A.M., "3D Navier-Stokes Computations in Transonic Compressor Bladings", Proceedings of the Xth ISABE Symposium edited by F.S. Billig, AIAA Washington D.C. (1991)

[2] Vuillot A.M., Couaillier V., Liamis N. "3D Turbomachinery Euler and Navier-Stokes Calculations with a Multidomain Cell-Centered Approach" AIAA/SAE/ASME/ASEE 29th Joint Propulsion Conference (1993)

[3] Lerat A., Sides J;, Daru V. "An Implicit Finite Volume Method for Solving the Euler Equations" Lecture Notes in Physics, vol 170 pp343-349 (1982)

[4] Balwin B.S., Lomax H. "Thin Layer Approximation and Algebraic Model for Separated Turbulent Flows" AIAA paper 78-257 (1978)

[5] Malecki R., Lord W. "Navier-Stokes Analysis of a Lobed Mixer and Nozzle" AIAA paper 90-0453 (1990)

[6] Yuan Jing Qiu "A Study of Streamvise Vortex Enhanced Mixing in Lobed Mixer Devices" Thesis, Massachusetts Institute of Technology June 1992

[7] Erikson L.E. "Generation of Boundary Conforming Grids Around Wing-Body Configurations Using Transfinite Interpolations" AIAA Journal vol 20 n°10 (1982)